Chain Dynamics of Poly(dimethylsiloxane) in the Intermediate Range

Fabio Ganazzoli,† Giuseppe Allegra,*† Julia S. Higgins,‡ Jaan Roots,§ Sergio Brückner,† and Emilio Lucchelli†

Dipartimento di Chimica del Politecnico, Piazza Leonardo da Vinci 32, 20133 Milano, Italy, Department of Chemical Engineering and Chemical Technology, Imperial College, London SW7 2BY, U.K., and Kjemisk Institut University of Oslo, Blindern, Oslo 3, Norway.
Received April 20, 1984

ABSTRACT: Quasi-elastic neutron scattering results obtained from poly(dimethylsiloxane) (PDMS) samples in C_6D_6 solution as well as from data on PDMS melts published by others in the range $0.026 < Q$ ($=4\pi \sin(\vartheta/2)/\lambda$) < 0.31 Å^{-1} are compared with a theoretical approach where the actual conformational properties of the chain are considered instead of the classical bead-and-spring model. Calculations account for the intramolecular elastic energy, for the hydrodynamic interaction short of the Zimm limit, and for the good-solvent effect; in view of the small rotational energy barriers, the internal viscosity has been neglected. Agreement between the calculated and the experimental dynamic coherent structure factor $S_{coh}(Q,t)$ is satisfactory. In agreement with previous results, PDMS appears to be a very flexible chain, which in turn is due both to conformational reasons (i.e., the broad-peaked generalized characteristic ratio) and to the absence of internal viscosity. Comparison between PDMS, polyethylene (or its stereochemically similar poly(tetrahydrofuran)), and atactic polystyrene shows the three polymers to possess an increasing rigidity. This is shown to be related both with a decreasing value of the exponent for the power law $t_c Q^{\beta} \simeq$ constant (t_c = characteristic time of $S_{coh}(Q,t)$) and with a smaller upward curvature of the line profiles of log $S_{coh}(Q,t)$ vs. t at fixed Q.

1. Introduction

As is well-known, the dynamical properties of an isolated polymer chain depart from a universal behavior when investigated over sufficiently short distances;[1] generally speaking, we may ascribe their specific features to the actual degree of chain rigidity.[2] Referring first to a relatively rigid polymer, quasi-elastic neutron scattering data from atactic polystyrene (PS) solutions in the intermediate range $0.04 < Q$ ($=4\pi \sin(\vartheta/2)/\lambda$) < 0.27 Å^{-1} were recently analyzed in the light of a general theoretical approach (ref 3, hereafter referred to as paper 1). The intramolecular rigidity was attributed to two distinct sources: (i) the rather extended equilibrium conformations, producing a relatively large value of the characteristic ratio ($C_\infty \simeq 10$) together with a sharp peaked generalized function $C(q)$ (conformational rigidity); (ii) the rather large free energy barriers hindering the rotational transitions around chain bonds (rigidity from internal viscosity); the latter effect is compounded with the solvent friction.[4,5]

In the present paper we will report the results of a similar analysis of the quasi-elastic neutron scattering data obtained by some of us (J.S.H. and J.R.) on poly(dimethylsiloxane) (PDMS), which may be regarded as a flexible polymer, in that both the above sources of rigidity should give a modest contribution (see the following discussion). The Q range investigated ($0.026 < Q < 0.31$ Å^{-1}) is only slightly wider than that adopted in paper 1 with PS, which enables us to carry out a comparison between the two polymers. In terms of the observation distance d, the above range may be roughly translated as $100 > d > 10$ Å,[6] wherein the individual atoms obviously cannot be recognized and the chain appears as a kind of a tube or worm with a specific degree of flexibility.[7] Under these conditions the dynamic coherent structure factor $S(Q,t)$ may be interpreted in terms of Gaussian-distributed correlation functions between all the pairs of chain atoms, provided the time t is sufficiently large.[2]

It must be recalled that the dynamic solution properties of PDMS were already investigated by one of us (J.S.H.) in a previous paper, using a more limited set of experimental data; the classical bead-and-spring model was adopted and the mean-square distance between neighboring beads was optimized to fit the data.[8] It should be stressed that the present approach adopts a molecular model of the chain wherein the conformational statistics is properly taken into account, while the scattering power is evenly concentrated on the chain atoms.[3] The excluded-volume effect[9] and the hydrodynamic interaction (coupled together through the interatomic distances appearing in the preaveraged Oseen tensor) as well as the internal viscosity[4] may also be accounted for in a self-consistent way, enabling the full evaluation of both the $S(Q,t)$ line shapes at constant Q as well as the corresponding characteristic times. However, in view of the low energy barriers for the rotations around the Si–O bonds,[10] the internal viscosity will be disregarded in the present case.[4]

Table I
PDMS Sample Characteristics (C_6D_6 Solution)

sample	M_w	C, %	T, °C	spectrometer
1a	174 000	3	30	IN11
1b	174 000	3	70	IN11
2	15 000	3	30	IN11
3	15 000	3	20	IN10

After the Experimental Section, we will briefly recall the theoretical background already given in paper 1, defining also the numerical value of the parameters. Then the experimental and calculated results will be discussed in comparison with other experimental[3,11] and theoretical[3,4] results previously obtained on different polymers. While our experimental data on PDMS were obtained from dilute solution in C_6D_6 (see Table I), some data obtained by other authors[12] from molten samples of the same polymer will also be considered.

The scattering ranges were selected to probe essentially intramolecular motions, avoiding as far as possible intermolecular (e.g., reptation) effects.

2. Experimental Section

The dynamic structure factor of PDMS in dilute solution in deuterated benzene was observed for two narrow molecular weight fractions at several temperatures and by using two high-resolution

† Dipartimento di Chimica del Politecnico.
‡ Imperial College.
§ Kjemisk Institut University of Oslo.

0024-9297/85/2218-0435$01.50/0

spectrometers. The different measurements are summarized in Table I.

One sample of relatively high molecular weight (174 000) was obtained directly from Midland Silicones. The other sample of low molecular weight (15 000) was prepared at the University of York following procedures already reported.[13] Data for this sample have already been published.[8] For neutron measurements these samples were dissolved in 3% solution in C_6D_6 and contained in thin-walled cans. For the IN11 spectrometer these were quartz for ambient-temperature measurements and niobium for the higher temperature. For the IN10 spectrometer aluminum was used.

The details of the neutron experiments have been described elsewhere[8,14] so that only a few important points will be mentioned here. IN11[15] is a neutron spin-echo spectrometer[16] and because the measurement keeps track of the neutron spin a clean separation of coherent scattering from incoherent scattering is possible. For this series of measurements therefore we report the pure dynamic coherent structure factor $S_{coh}(Q,t)$. The technique also gives results directly in the time domain, by essentially counting the precessions of the neutron spin in a magnetic field. Inhomogeneities in this magnetic field eventually limit the accessible time scale to between 10^{-9} and 10^{-8} s. The corresponding Q range lies above 0.02 Å^{-1} and is limited at its upper end by lack of intensity in the coherent structure factor. In practice results have not been obtained for $Q > 0.132$ Å^{-1}.

The backscattering spectrometer, IN10,[15] is based on an entirely different technique. A 180° Bragg reflection from silicon single crystals gives a sharply defined energy which is then scanned with a Doppler drive. The spectrometer thus observes the Fourier transform of $S(Q,t)$ in the frequency domain, $S(Q,\omega)$. The limiting energy resolution is 1 μeV and we report data for $Q > 0.15$ Å^{-1}. For this spectrometer no experimental separation of the incoherent and coherent scattering from the sample is possible, and since the coherent structure factor at $t = 0$ becomes quite small with increasing Q, unlike the incoherent structure factor which is constant with Q, the data are a mixture of the coherent and incoherent components. However, even for the highest Q value (=0.31 Å^{-1}) reached in our investigation, the ratio $S_{inc}(Q,0)/S_{coh}(Q,0)$ is always below 0.1, the relatively large coherent factor being essentially due to the contrast with the C_6D_6 solvent. Consequently, since the time decays of S_{inc} and S_{coh} are about the same, we will regard our dynamic structure factor results as essentially coherent.

The frequency data have been Fourier transformed to give $S(Q,t)$ ($\simeq S_{coh}(Q,t)$) to enable comparison with the calculated correlation functions. A discussion of the relationship between $S(Q,t)$ and $S(Q,\omega)$ is given by Heidemann et al.[17] The procedure adopted for obtaining $S(Q,t)$ from IN10 data is given in a report by Howells.[18] Data are first corrected for can scattering, self-absorption, etc., in the usual way. A fast Fourier transform of the sample and resolution experiments is made and the sample $S(Q,t)$ is obtained by dividing the two FT spectra. The standard deviations are computed for the Fourier coefficients from the statistical noise on the original data. The function $S(Q,t)/S(Q,0)$ should be unity at $t = 0$, so the data have been renormalized by using visual extrapolation to obtain $S(Q,0)$. This procedure is necessary because of the possibility of a residual flat background which Fourier transforms to a δ function at the origin. The limited frequency range available experimentally also means that the FT data must be treated with some caution.

3. Theoretical Method

In paper 1 it was shown that an $[-A-B-]_N$ chain may be described as an equivalent, suitably defined $[-A'-]_{2N}$ chain, provided the observation length is sufficiently large. Accordingly, we will discuss in the following the most important configurational[19] and dynamical factors and the related parameters required to perform the calculations.

3.1. Generalized Characteristic Ratio $C(q)$. This is a function of the Fourier configurational mode coordinate q[20] which contains all the information both on the mean-square intramolecular distances and on the intramolecular elastic forces, provided we assume the molecules are in the unperturbed state and within the linear approximation for the dynamic equations. In particular, the longer the range of correlation between successive bonds, the sharper is the origin peak of $C(q)$. $C(0)$ is the usual characteristic ratio C_∞, apart from a relatively small correction arising from incomplete suppression of the intramolecular repulsions even at the Θ-temperature.[21] The mean-square distance between two chain atoms separated by k bonds is given by

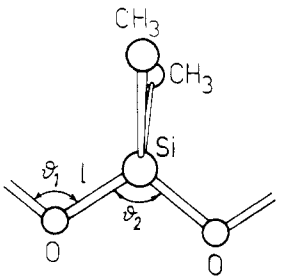

Figure 1. Schematic drawing of PDMS showing the geometrical parameters l, ϑ_1 and ϑ_2 (see Table II).

$$\langle r^2(k)\rangle = \frac{l^2}{2N}\sum_{\{q\}}\frac{\sin^2(qk/2)}{\sin^2(q/2)}C(q) \qquad (1)$$

where $\{q\} = 0, \pm\pi/N, \pm 2\pi/N, ..., \pm\pi$, and N and l are the total number of monomeric units and the length of each chain bond, respectively. In paper 1 we showed how to obtain $C(q)$ within the rotational-isomeric-state (ris) approximation for a polymer with a random distribution of stereoisomeric centers (see eq 29, paper 1)

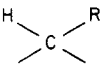

The same procedure may be easily modified to accommodate the configurational description of Flory, Crescenzi, and Mark.[22] It suffices to identify the matrices $\mathbf{U}'$ and $\mathbf{U}''$ of eq 25, paper 1, with $\mathbf{U}'$ and $\mathbf{U}''$ of ref 22, while suitably constructing Ψ_1 and Ψ_2 (eq 25, paper 1) with the 3×3 matrices $\mathbf{T}(\varphi_k,\vartheta_h)$ (eq 27, paper 1) performing the allowed rotations φ_k with the appropriate bond angles ϑ_h ($h = 1$, 2, see Figure 1 and Table II). We also carried out analogous calculations considering all the skeletal rotations (asr approach[23,24]), using the conformational energy parameters proposed by one of us in a paper where the ris and asr approaches were comparatively discussed for the specific case of PDMS.[10] The algorithm to obtain $C(q)$ is easily derivable from that reported in paper 1 by mere isomorphic substitution of all the ris matrices with the corresponding ones in the asr language, as discussed in ref 25. The $C(q)$ functions obtained with either approach are reported in Figure 2. Their close resemblance stresses once again the remarkable agreement between the two approaches that may be obtained if the energy parameters are properly chosen. (It is to be pointed out, however, that a suitably optimized asr scheme represents in general a more realistic approximation; as an example, the plots of the intramolecular distribution functions $W(r)$ obtained for PDMS with an ris Monte Carlo approach show a typical discontinuous unphysical behavior which is not displayed by the corresponding asr plots; see Figure 6 of ref 10.) For expediency, we have approximated the average of the two resulting functions with the analytical relationship[21]

$$C(q) = \frac{a}{1 - b\cos q} + c \qquad (2)$$

the parameters a, b, and c being reported in Table II. Although our calculations were carried out at 350 K (77

Table II
Physical Parameters Used in the Calculations

symbol	defin or eq	value	source
l	Si-O bond length	1.64 Å	ref 26, chapter 5, section 10
ϑ_1	∠Si-O-Si bond angle	143°	
ϑ_2	∠O-Si-O bond angle	110°	
$C(q)$ a	eq 2	0.4312	present work, from calculation
$C(q)$ b		0.9320	
$C(q)$ c		−0.1521	
h_0	eq 6	0.04 (in melts, 0.0)	present work, from diffusion data of oligomers[35]
$\bar{\beta}$	eq 10, 17 of ref 9	0.25 (in melts, 0.0)	present work, from expansion data[29]
R_{eff}	eq 14	0.30 ± 0.04 Å	present work, best fit from scattering data
$2N$	no. of skeletal atoms	samples 1a, b, $2N$ = 5000	
		samples 2, 3, $2N$ = 400	from Table I and ref 12
		melt, $2N$ = 1600	

		value			
		solution (C_6D_6)			
symbol	defin or eq	T = 30 °C	T = 70 °C	melt (T = 100 °C)	source
η_s	solv viscosity	0.604×10^{-2} P	0.369×10^{-2} P		from ref 42
ζ	eq 6	$(3.4 \pm 0.5) \times 10^{-10}$ g s^{-1}	$(2.0 \pm 0.3) \times 10^{-10}$ g s^{-1}	$(9.2 \pm 0.6) \times 10^{-9}$ g s^{-1}	present work
t_0	eq 12	$(2.2 \pm 0.3) \times 10^{-12}$ s	$(1.2 \pm 0.2) \times 10^{-12}$ s	$(4.8 \pm 0.3) \times 10^{-12}$ s	present work

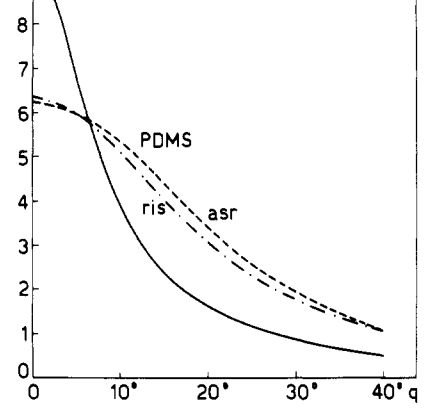

Figure 2. Plot of $C(q)$ for PDMS at T = 350 K as calculated in the rotational isomeric scheme (ris) approximation and accounting for all skeletal rotations (asr) (see text). For sake of comparison, the $C(q)$ of a more rigid polymer, i.e. polystyrene (PS) is also reported (from ref 2).

°C), we have assumed the same results to be valid at room temperature as well.[22,26]

3.2. Internal Viscosity. This effect is assumed as arising from hindrance to skeletal rotations.[4] Although the friction with the solvent appears to be an important cofactor,[27] we have decided to neglect the internal viscosity in view of the extremely small intramolecular energy barriers, if any, existing between the accessible rotational states[10] (note that steric hindrance between side groups of neighboring monomeric units is unlikely, especially because of the large bond angle at the oxygen atom; see Figure 1 and Table II). The above assumption appears to be confirmed by recent experimental results.[28]

3.3. Good-Solvent Expansion. Following paper 1, we have taken care of this effect by introducing an "effective" value of $C(q)$

$$C_{eff}(q) = C(q)\tilde{\alpha}^2(q) \tag{3}$$

where $\tilde{\alpha}^2(q)$ is the mean-square expansion factor for the q-configurational mode. To evaluate this function we need the (adimensional) excluded-volume parameter per chain atom $\bar{\beta}$. In an investigation of linear and cyclic PDMS of varying length dissolved in toluene at 25 °C Edwards, Stepto, and Semlyen[29] give, inter alia, the diffusion-related (α_f) and viscosity-related (α_η) expansion factor of two linear fractions with a known number average of chain bonds $\bar{n}_n$ (L8 and L9, Table 2 of ref 29). Elaboration of these data through the equations

$$\alpha_f \simeq 1 + 0.609z; \qquad \alpha_\eta \simeq 1 + 0.517z \tag{4}$$

proposed by Yamakawa[30] and reported in the quoted paper[29] gives four independent z values. From the correspondence (see Figure 1 of ref 9, $k \rightarrow \bar{n}_n$)

$$\bar{\beta} = {}^4/_3 z(\bar{n}_n)^{-1/2} \tag{5}$$

we get figures of $\bar{\beta}$ between 0.02 and 0.03, the average of which is reported in Table II ($\bar{\beta}$ = 0.025). As done in paper 1, the mean-square expansion factor $\tilde{\alpha}^2(q)$ was then obtained from Figure 1 of ref 9.

Unlike the case of the solution samples, the polymer chains were regarded as unperturbed in the molten state, so that no expansion correction was applied (i.e., $\tilde{\alpha}^2(q) \equiv 1$). This is in agreement both with Flory's theoretical predictions on thermodynamic grounds[31] and with the experimental findings (see ref 32, e.g.).

3.4. Hydrodynamic Interaction. The effects of hydrodynamic interactions were taken care of in the preaveraged approximation via a q-dependent friction coefficient per chain atom, i.e.[33,34]

$$\zeta(q) = \zeta/(1 + h_0 f(q)) \tag{6}$$

where $f(q)$ is a suitably normalized Fourier transform of $\langle r^{-1}(k)\rangle$

$$f(q) = \pi(2N)^{1/2} \sum_{k=1}^{2N} (2N - k) \cos(qk) \times \langle r^{-1}(k)\rangle / \sum_{k=1}^{2N} (2N - k)\langle r^{-1}(k)\rangle_0$$

$$= \pi R_{H_0}(2N)^{-3/2} \sum_{k=1}^{2N} (2N - k) \cos(qk)\langle r^{-1}(k)\rangle \tag{7}$$

in which R_{H_0} is the unperturbed hydrodynamic radius, while the hydrodynamic parameter h_0 is (see eq 20 of paper 1)

$$h_0 = \frac{\zeta}{3\pi^2\eta_s}\frac{(2N)^{1/2}}{R_{H_0}} \simeq \frac{4}{9\pi^2}\left(\frac{6}{\pi C(0)}\right)^{1/2}\frac{1}{l}\frac{\zeta}{\eta_s} \tag{8}$$

ζ and η_s being the friction constant per chain atom and the solvent viscosity, respectively. Within the Gaussian ap-

proximation, the reciprocal average $\langle r^{-1}(k)\rangle$ is related with $\langle r^2(k)\rangle$ (see eq 1) by

$$\langle r^{-1}(k)\rangle = [6/\pi\langle r^2(k)\rangle]^{1/2} \tag{9}$$

It should be stressed that the reciprocal average $\langle r^{-1}(k)\rangle$, hence $f(q)$ and $\zeta(q)$, are evaluated through the actual, perturbed value of $\langle r^2(k)\rangle$. In this way the expansion of the chain due to the good solvent is indirectly reflected in a decrease of the hydrodynamic interaction.

We established an approximate figure for h_0 from a previous investigation on the hydrodynamic radii R_H of linear PDMS chains.[35] We got $\zeta/\eta_s \simeq 2.9 \times 10^{-8}$ cm using the data referring to the shortest chains ($2N < 75$) and the Stokes–Einstein equation

$$D = \frac{k_B T}{6\pi\eta_s R_H} \simeq \frac{k_B T}{N\zeta} \tag{10}$$

where the last approximate equality stems from the consideration that we expect the hydrodynamic interaction to be essentially ineffective for these short chains. By substitution of the above value into eq 8 we get $h_0 \simeq 0.04$. Of course, for the molten sample we put $h_0 = 0$ in view of the hydrodynamic screening exerted by the surrounding chains.[33]

The numerical value of the parameters is reported in Table II.

4. Dynamic Coherent Structure Factor

We are able now to obtain the space–time correlation function for sufficiently long times t (see eq 22 and 22′ of paper 1, $q \ll 1$)

$$B(k,t) = \langle[\mathbf{r}(k,t) - \mathbf{r}(0,0)]^2\rangle = \frac{l^2}{2N}\sum_{|q|}\frac{2C_{eff}(q)}{q^2}\{1 - e^{-t/\bar{\tau}(q)}\cos(qk)\} \tag{11}$$

where $\mathbf{r}(k,t)$ is the vector position of the k-th atom at time t and

$$\bar{\tau}(q) = t_0\frac{C_{eff}(q)}{3q^2}\frac{1}{1 + h_0 f(q)}; \qquad t_0 = \frac{\zeta l^2}{k_B T} \tag{12}$$

(Here and in the following we assume $t \gg t_0$.[2]) The dynamic coherent structure factor of an N-monomeric unit chain the monomer of which consists of two skeletal atoms is[36]

$$S_{coh}(Q,t) = (2N)^{-1}\left\{\exp\left[-\frac{Q^2}{6}B(0,t)\right] + 2\sum_{k=1}^{2N}\left(1 - \frac{k}{2N}\right)\exp\left[-\frac{Q^2}{6}B(k,t)\right]\right\} \tag{13}$$

where

$$Q = 4\pi \sin(\vartheta/2)/\lambda$$

5. Results and Discussion

5.1. Line Profiles vs. t and Characteristic Times of PDMS. The calculated and experimental dynamic structure factor plots are reported in Figure 3. Although for the solution samples the time unit t_0 (eq 12) may be obtained from the previous estimate of ζ/η_s (eq 10), as done in paper 1 we considered the effective value of ζ as an adjustable parameter, in view of the approximations involved. However, a Stokes-type equation was used to correlate ζ/η_s with the effective radius per chain atom R_{eff} (reported in Table II)

$$\zeta/\eta_s = 6\pi R_{eff} \tag{14}$$

In practice, we fitted the calculated half-peak times $t_{1/2}$

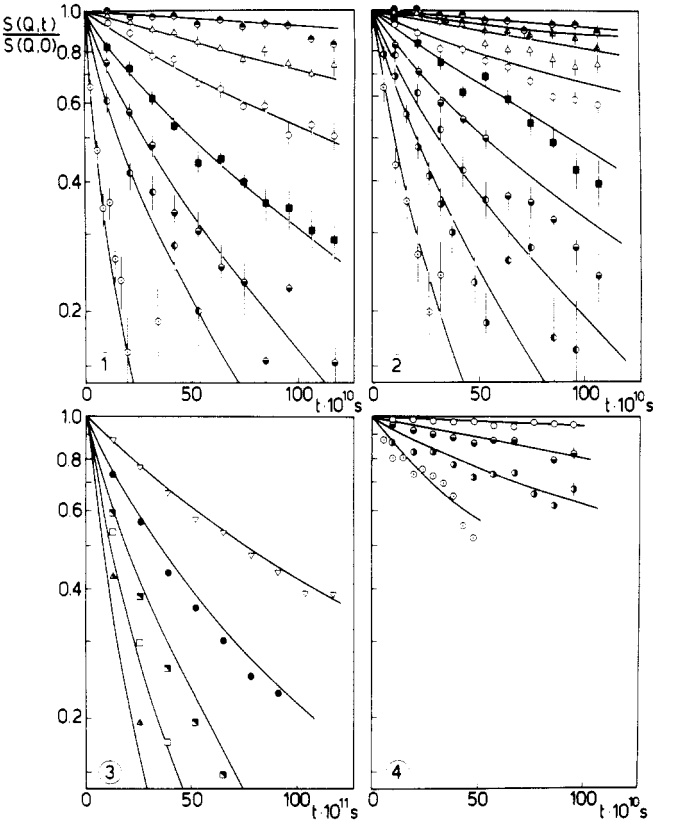

Figure 3. Experimental points and calculated curves of $S_{coh}(Q,t)$ vs. t for different Q values. Parts 1–3 correspond to samples 1–3 of Table I, where sample 1b is scaled from $T = 30$ °C to $T = 70$ °C through the ratio η_s/T. Part 4 is from ref 12. The Q values are as follows: (⊖) 0.0264, (▲) 0.0330, (△) 0.0396, (○) 0.0528, (■) 0.0660, (◒) 0.0792, (◐) 0.0924, (◑) 0.1056, (⊙) 0.1320, (▽) 0.15, (●) 0.19, (◘) 0.23, (□) 0.27, (▲) 0.31 Å^{-1}.

to the experimental data by adjusting a single parameter R_{eff} to all the curves shown in Figure 3, parts 1–3, hence ζ (through eq 14) and t_0 (through eq 12). Concerning the molten sample, we adjusted separately ζ, hence t_0 (Figure 3, part 4).

As usual, the overall dependence of $S(Q,t)$ from Q has been expressed in terms of a characteristic time $t_c(Q)$. While t_c has been identified with the half-peak time $t_{1/2}$ for the solution samples,[2] we decided to rely on the three-fourths peak time $t_{3/4}$ (i.e., $S(Q,t_{3/4}) = {}^3/_4 S(Q,0)$) for the melt, to avoid the experimental limitations of the spin-echo technique which does not permit observation of very long times.[16] The characteristic times are reported vs. Q in Figure 4. Within appropriate ranges of Q, the power law

$$t_c Q^{\mathcal{B}} \simeq \text{constant} \tag{15}$$

may be adopted, the resulting value of the exponent $\mathcal{B}$ being reported in Table III. The agreement between the calculated and observed values appears to be good for both the solution and the melt samples.

It may be observed that for the solutions the $\mathcal{B}$ exponent decreases from values in the range 3.2–3.4 for the lower Q's (slightly depending on M_w) to about 2.6 for $Q \gtrsim 0.15$ Å^{-1}. As is apparent from Table III, although the agreement with our calculated exponent is generally good, it becomes rather poor in this upper Q range ($\mathcal{B}_{calcd} = 3.2$, $\mathcal{B}_{expti} = 2.6$). On the other hand, inspection of Figure 4, left-hand side, shows that the decrease of the average slope of log $t_{1/2}$ vs. log Q at higher Q's is only suggested by the two last experimental points. It should be noted that, for these two experimental points, the overall energy range of our

Table III
Average Power Law Exponent $\mathcal{B}$ for the Equation $t_c Q^{\mathcal{B}} \simeq$ Constant for Different Ranges of Q^a

sample no.	exptl	calcd
	Solution Data ($t_c \equiv t_{1/2}$)	
1a,b[b]	3.4 ± 0.1 (0.05 < Q < 0.11 Å^{-1})	3.28 (0.05 < Q < 0.15 Å^{-1})
2	3.2 ± 0.1 (0.065 < Q < 0.13 Å^{-1})	3.22 (0.06 < Q < 0.15 Å^{-1})
3	2.6 ± 0.3 (0.15 < Q < 0.31 Å^{-1})	3.22 (0.15 < Q < 0.31 Å^{-1})
	Melt Data, T = 100 °C ($t_c \equiv t_{3/4}$)	
from ref 12 and Figure 3, section 4	4.0 ± 0.1 (0.08 < Q < 0.13 Å^{-1})	4.03 (0.05 < Q < 0.15 Å^{-1})
		3.58 (0.15 < Q < 0.31 Å^{-1})

[a] Coherent scattering, eq 15. [b] $t_{1/2}$ time for sample 1b (see Table I) is scaled from 30 to 70 °C through the ratio η_s/T.

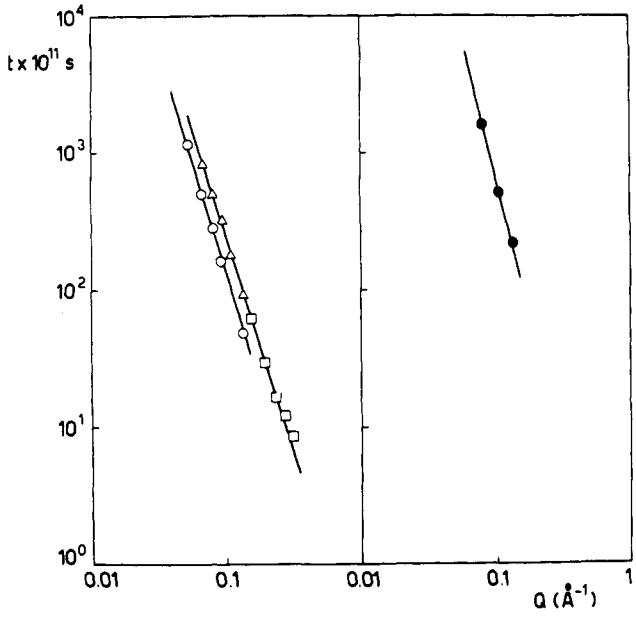

Figure 4. Characteristic times t_c plotted vs. Q. Left ($t_c \equiv t_{1/2}$): the lower curve is the theoretical result at T = 70 °C, the upper curve at T = 30 °C. The points indicated as ○, △, and □ refer to samples 1–3, respectively (see Figure 3 and Table I); sample 3 is scaled from T = 20 to T = 30 °C through the ratio η_s/T. Right ($t_c \equiv t_{3/4}$): The calculated curve is for melts at T = 100 °C. The points indicated as ● are from ref 12 (see also Figure 3).

measurements appears to be rather close to the limits where intensity is still detectable. Obviously, any failure to account for intensity in the ω tails leads to a lower estimate of $S(Q,0)$ and consequently to a longer $t_{1/2}$.

The R_{eff} value deduced via ζ from the time-scale fitting of solution data through eq 12 and 14 is ≃0.30 Å and may be compared with value of ≃0.4 Å for PS.[3] It must be stressed that the ζ/η_s value obtained in section 3.4 from the diffusion data of oligomers gives $R_{eff} \simeq$ 0.15 Å, which is close to the value 0.125 Å obtained from h_0 in the case of PS. Again, as done in paper 1, these very small and poorly consistent values of R_{eff} may be traced back to some inadequacy of Stokes' law when the solvent molecular mass and the effective polymer mass are roughly equal (see also ref 37 and the discussion in paper 1).

When we refer to the melt data, the ζ value obtained from the time-scale fitting, i.e., (9.2 ± 0.6) × 10^{-10} g s^{-1}, is in fair agreement with the value of 1.41 × 10^{-9} g s^{-1} obtained by Ferry[38] from dynamical mechanical measurements.

5.2. Conformational Rigidity and Internal-Viscosity Rigidity. A Comparison with Other Polymers. In principle, if measured under comparable conditions, the $\mathcal{B}$ exponent of a flexible polymer should be larger than that of a rigid polymer. This conclusion may be obtained through a theoretical analysis of the Fourier normal modes of a realistic model,[2] possibly including the internal viscosity;[4] it was also reached with the aid of a bead-and-spring model where the average spring length is assumed to be roughly proportional to the chain rigidity.[39]

We shall first perform a comparison among PDMS, PE (polyethylene), and PS (atactic polystyrene). These polymers should display in the quoted order an increasing rigidity; comparing PDMS with PE, this should be mainly due to conformational reasons, while the internal viscosity should be the dominant factor for the higher rigidity of PS with respect to PE. Limiting ourselves to calculated data, we will compare the $t_{3/4}$ time of the coherent structure factor of the molten polymers, to avoid both the hydrodynamic interaction and the excluded volume; entanglement effects will be disregarded. Actually, the comparison should be done for corresponding values of Q, and to this effect we must take into consideration the difference between the bond lengths and angles of PDMS (see Figure 1) and those of the hydrocarbon-type polymers. To scale Q according to the molecular size which is invariant under backbone rotations, we used the following method. After calculating the mean-square length of the freely rotating model $\langle L_{fr}^2 \rangle$ (with fixed bond angles and lengths) we obtained the bond length of the equivalent freely jointed chain, $l_n = (\langle L_{fr}^2 \rangle / 2N)^{1/2}$; then we took Ql_n as the scaled value of Q. Specifically, if l is the backbone bond length and ϑ_1 and ϑ_2 are the bond angles per monomeric unit, the mean-square end-to-end distance of the freely rotating chain with $2N$ bonds is (see ref 26, chapter I, eq 24)

$$\langle L_{fr}^2 \rangle = 2Nl_n^2 = 2Nl^2(1 - \cos\vartheta_1)(1 - \cos\vartheta_2)/(1 - \cos\vartheta_1 \cos\vartheta_2) \quad (16)$$

Taking for PDMS the geometrical parameters given in Figure 1 and Table II while for both PE and PS $\vartheta_1 = \vartheta_2 = 111°$, l = 1.54 Å, we get

$$l_n(\text{PDMS}) = 2.99 \text{ Å}; \qquad l_n(\text{PE,PS}) = 2.24 \text{ Å} \quad (17)$$

Figure 5 shows the logarithmic calculated plots of $t_{3/4}(Ql_n)^2$ vs. the normalized variable Ql_n for the three polymer melts (i.e., $h_0 = 0$, $\bar{\beta} = 0$) within a range approximately corresponding to 0.1 < Q < 0.4 Å^{-1}; the resulting slopes are obviously equal to $\mathcal{B} - 2$ (see eq 15, where $t_c = t_{3/4}$). For the sake of comparison, the time scales were shifted so that the three curves merge at lower Q. As expected, for any value of the abscissa the exponent $\mathcal{B}$ decreases in the order PDMS → PE → PS. (If the unnormalized coordinate Q were used, there would be an inversion at higher Q's between PDMS and PE.) Since the internal viscosity parameter τ_0[4] was equated to zero for both PDMS and PE, the difference between these two polymers is merely due to the higher conformational rigidity of the latter, as anticipated. Approximate measures of this rigidity are provided either by the reciprocal of the half-peak half-width (hphw) of the function $C(q)$ (21.2° for PDMS and 11.4° for PE) or by the ratio of C_∞ (≃$C(0)$) to the corre-

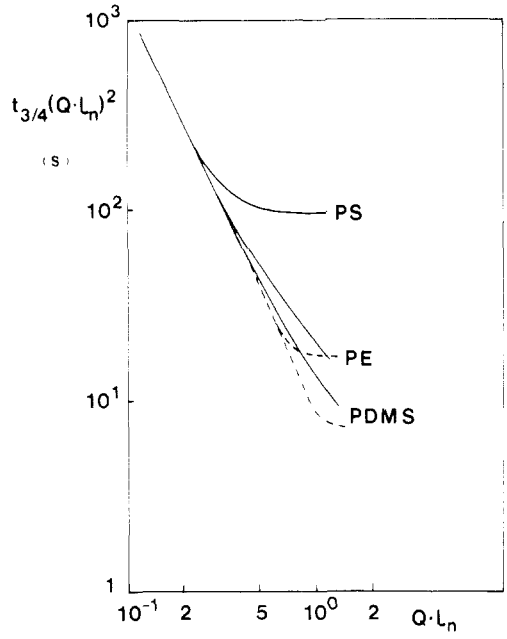

Figure 5. Calculated characteristic time $t_{3/4}$ plotted as $t_{3/4}(Q\cdot l_n)^2$ vs. the normalized wave vector $Q\cdot l_n$ for PDMS, PE, and PS melts ($h_0 = 0$; $\bar{\beta} = 0$, solid lines). The time unit for PDMS corresponds to t_0 (see eq 12 and Table II), while the curves of PE and PS have been shifted so that the three curves merge at low Q. The dashed lines correspond to the Rouse bead-and-spring models equivalent to PE and PDMS, with a root-mean-square distance between neighboring beads of 12.8 and 11.5 Å, respectively (see text).

sponding value C_∞(fr) of the freely rotating chain (i.e., 1.88 for PDMS and 3.24 for PE). On moving to PS, we find a further increased conformational rigidity (i.e., 8.4° as the hphw of $C(q)$, or 4.37 as C_∞/C_∞(fr)) together with the internal-viscosity effect, and we know that the latter accounts for most of the difference.[3] (In view of the illustrative character of these calculations, for simplicity τ_0 of PS was taken at 30 °C.)

In the same figure, two dashed lines show the behavior of the Rouse model for the two polymers wherein the internal viscosity is considered to be absent, namely PE and PDMS, constructed in such a way that the length L of the Kuhn's statistical segment is identical with the root-mean-square distance between neighboring beads. (Determination of L was carried out according to the equation $L = C(0)l/\langle\sin(\vartheta/2)\rangle$, where the brackets are required only in the case of PDMS and imply arithmetic average over ϑ_1 and ϑ_2. This equation may be derived from eq 18 of ref 26, Chapter I, considering—upon use of appropriate geometric models—that the conformations enabling maximum extension of the PDMS chain bring the O → O and Si → Si vectors between nearest-neighboring atoms virtually parallel to the chain axis.) Using 6.9 and 6.2 as C_∞ for PE and PDMS, respectively, we get $L_{PE} = 12.8$ Å, $L_{PDMS} = 11.5$ Å. As already shown in Figure 4 of ref 2 in terms of $B(0,t)$ vs. t, the Rouse model appears to be more flexible than the real one at small Q (i.e., larger slope), until it suddenly tends to $\mathcal{B} \simeq 2$ where Q is large enough to probe the diffusion of the separate beads. Otherwise said, the Rouse model becomes completely unrealistic within the higher Q domain.

Incoherent neutron scattering results previously reported by one of us, with co-workers, on several polymer melts (i.e., PDMS, a few polyethers and polyisobutylene)[11] may also provide interesting semiquantitative comparison with the present results. These data were obtained in the frequency domain as $S(Q,\omega)$. The values of $\mathcal{B}$ are evaluated by extracting the full width at half-maximum, $\Delta\omega$, and

Table IV
$\mathcal{B}$ Exponent for Incoherent Scattering for Different Polymers at Several Temperatures[a]

polymer[b]	T, °C	$\mathcal{B}$(exptl)	$\mathcal{B}$(calcd)
PDMS	20	4	3.35 (Q = 0.25 Å^{-1}, T = 77 °C)
	150	4	
PPO	67	3.0	
	150	3.4	
PTHF	73	3.1	3.10 for PE (Q = 0.4 Å^{-1}, T = 127 °C)
	150	3.5	
PEO	68	3.2	
PIB	73	2.2	
	150	2.9	

[a] The Q range is centered at 0.5 Å^{-1} for the experimental values (from ref 11). [b] PDMS = poly(dimethylsiloxane), PPO = poly(propylene oxide), PTHF = poly(tetrahydrofuran), PEO = poly(ethylene oxide), PIB = polyisobutylene.

assuming a dependence $\Delta\omega = K\cdot Q^{\mathcal{B}}$. In order to extract $\Delta\omega$ from the instrumental resolution, a model $S(Q,\omega)$ is used; in this case the model was that for pure Rouse motion. As shown in Table IV, the largest experimental value of the exponent $\mathcal{B}$ around $Q = 0.5$ Å^{-1} corresponds to PDMS. Assuming the polyethers to behave roughly as PE, the result agrees quantitatively with our calculations; the discrepancy between the experimental and calculated $\mathcal{B}$ values of PDMS is rather large, although with an opposite sign from that observed in the solution case within the higher Q range (see Table III, sample 3). (It should be stressed, in this context, that there seems to be no simple physical reason for significant differences between the dynamical behavior of a polymer solution and of a melt in this range of observation lengths, since according to our calculations both the hydrodynamic interaction and the excluded-volume effect tend to vanish for $Q \gtrsim 0.2$ Å^{-1}, as already verified for PS.[3,40]) Perhaps, as discussed in ref 8, interchain propagation modes may be partially responsible for this very large $\mathcal{B}$ value in the PDMS melts. It is interesting that no temperature effect is observed with this polymer, thus confirming our hypothesis that any energy-activated internal viscosity is essentially absent. Poly(tetrahydrofuran), of which PE appears to be a reasonable model, does indeed show a satisfactory agreement with the exponent previously evaluated by us for PE;[2] a moderate increase of $\mathcal{B}$ with temperature, also observed with poly(propylene oxide), is consistent with some internal-viscosity effect. It is remarkable that the largest temperature increase is observed with polyisobutylene, i.e., a polymer chain where the energy barriers between the rotational minima were roughly evaluated as >5 kcal/mol, due to a steric interference between methyl groups of adjacent monomeric units.[11,41] In spite of the lack of corresponding data for PS, we have calculated for this polymer roughly the same temperature variation of $\mathcal{B}$ as observed for PIB.

5.3. Difference between the Line Shapes of a Flexible (PDMS) and of a Rigid (PS) Chain. Comparative inspection of the ($S_{coh}(Q,t)$ vs. t) plots reported in Figure 3 of paper 1 and in Figure 3 of this paper shows that in the case of PS the time decay has some overall similarity with that of a single exponential (i.e., a straight line in the semilogarithmic plot), unlike the case of PDMS, where the upward concavity is much more evident. The trend is especially apparent for $Q > 0.1$ Å^{-1}; as an example, two plots are reported in Figure 6 for the same Q, one from each polymer, using two different time scales so that the experimental $t_{1/2}$ corresponds to the same abscissa. (It should be noted that the systematic misfit between the calculated lines and those through the experimental points

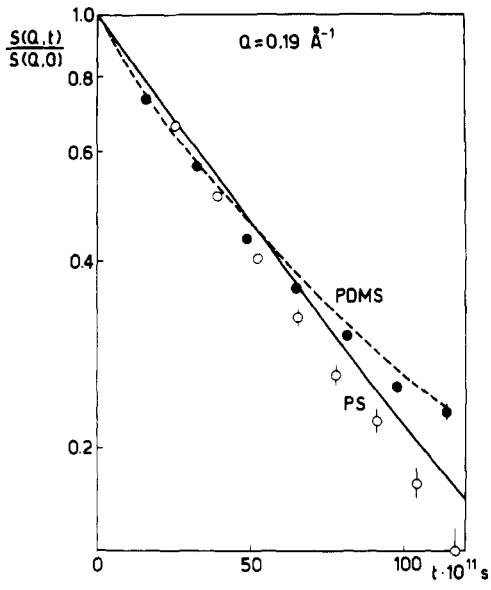

Figure 6. Experimental points and calculated curves of $S_{coh}(Q,t)$ at 30 °C plotted vs. t at $Q = 0.19$ Å^{-1} for PS (empty circles, CS_2 solution from ref 3) and PDMS (filled circles, present paper). The PDMS time unit has been scaled so that its experimental $t_{1/2}$ coincide with that of PS.

is due to our fitting with a single parameter all the $S_{coh}(Q,t)$ lines for a given polymer in solution.) As a quantitative measure of the difference between the two polymers in the range $0.19 < Q < 0.27$ Å^{-1}, the experimental ratio $t_{1/2}$:$t_{1/4}$ for PDMS is about 0.8 times the same ratio for PS. It should be pointed out that (i) the ratio is evaluated over three different plots for each polymer, in the above range, (ii) there is a good agreement between the values obtained either from the calculated lines or from fitting the experimental points, and (iii) the effect is seen even more clearly if we compare $S(Q,t)$ curves with the same normalized Ql_n value (see eq 17). This may be easily understood in a qualitative sense if attention is focused on the incoherent structure factor.[36]

$$\ln S_{incoh}(Q,t) = -\frac{1}{6}Q^2B(0,t) \quad (18)$$

If we remember that $B(0,t) \propto t^{2/\mathcal{B}}$, where the exponent changes with time very slowly,[2] the logarithmic time derivative of the above logarithm is ($d\mathcal{B}/dt = 0$)

$$t(\ln S_{incoh})^{-1}[\partial(-\ln S_{incoh})]/\partial t = \partial \ln(-\ln S_{incoh})/\partial \ln t = 2/\mathcal{B} \quad (19)$$

Although the theoretical analysis reported in ref 2 does not take into account the internal viscosity which for PS is a relevant factor, nevertheless the conclusions are valid in a qualitative sense. In the same paper, eq 34–51, it was shown that the time range wherein the value of the exponent $\mathcal{B}$ is larger than 2 (for $t/t_0 \gg 1$) and smaller than the Rouse value of 4 contracts more and more for flexible chains. As a result, with PDMS the $\mathcal{B}$ value reaches more quickly the terminal value of 4 than with PS, upon increasing t; consequently, the derivative reported in eq 19 gets smaller, as observed.

6. Concluding Remarks

In a previous paper partly due to one of us, PDMS was already shown to possess rather flat conformational energy maps and low barriers between conformers.[10] These two features are respectively related with the rapid loss of rotational correlation with increasing distance between skeletal bonds (conformational flexibility) and with a small degree of rotational hindrance (internal-viscosity flexibility) which in turn appear to be rather well demonstrated by the present study. Consequently, the dynamic flexibility of the PDMS chains, correlated with a large value (>3) of the $\mathcal{B}$ exponent (see eq 15), for $Q > 0.1$ Å^{-1}, is sharply larger than that of atactic polystyrene,[3] which is conformationally more rigid and appears to have a significant internal viscosity.[4] An intermediate case is represented by PE (see Figure 5), as is indirectly supported by previous experimental results on the stereochemically analogous poly(tetrahydrofuran). As shown in Table IV, this polyether, as well as the analogous poly(propylene oxide), appears to display some energy-activated internal viscosity; a still larger effect is observable with polyisobutylene (PIB), thus strongly suggesting a correlation between the spatial interference caused by the side groups of adjacent monomeric units (e.g., PS, PIB) and a large internal viscosity.[4]

In addition to the usual analysis of the characteristic times of the dynamic structure factor $S(Q,t)$ at different Q's, the line shape of $S(Q,t)$ at a given Q may provide useful information. As Figure 6 shows, the more flexible the polymer, the more pronounced is the upward concavity of the line, especially if the comparison is made between lines measured at the same normalized Q coordinate (see Figure 5).

As a final remark, we want to stress the fair amount of structural and dynamical information that may be gained on a given polymer if the conformational properties embodied in the $C(q)$ function and the possible internal-viscosity effect inherent with the skeletal rotations are considered, which is not allowed by the classical bead-and-spring model.

Acknowledgment. This study was made possible by a contribution from the Progetto Finalizzato per la Chimica Fine e Secondaria, Consiglio Nazionale delle Ricerche (Italy).

References and Notes

(1) de Gennes, P. G. "Scaling Concepts in Polymer Physics"; Cornell University Press: Ithaca, NY, 1979; Chapter 5.
(2) Allegra, G.; Ganazzoli, F. *J. Chem. Phys.* **1981**, *74*, 1310.
(3) Allegra, G.; Higgins, J. S.; Ganazzoli, F.; Lucchelli, E.; Brückner, S. *Macromolecules* **1984**, *17*, 1253 (also quoted as paper 1).
(4) Allegra, G.; Ganazzoli, F. *Macromolecules* **1981**, *14*, 1110.
(5) Kramers, H. A. *Physica* **1940**, *7*, 284.
(6) An approximate correlation between d and Q may be established as follows. Suppose the distance between two pointlike scatterers isotropically oriented is Gaussian distributed with a mean-square value d^2. Their integral scattered intensity vs. Q is $\propto Q^2 \exp(-\frac{1}{6}Q^2d^2)$ and is largest for $Q = 6^{1/2}/d$, which may be regarded as the correlation desired.
(7) Allegra, G. *J. Chem. Phys.* **1983**, *79*, 6382.
(8) Nicholson, L. K.; Higgins, J. S.; Hayter, J. B. *Macromolecules* **1981**, *14*, 836.
(9) Allegra, G.; Ganazzoli, F. *J. Chem. Phys.* **1982**, *76*, 6354.
(10) Brückner, S.; Malpezzi, L. *Makromol. Chem.* **1982**, *183*, 2033.
(11) Allen, G.; Higgins, J. S.; Maconnachie, A.; Ghosh, R. E. *J. Chem. Soc., Faraday Trans. 2* **1982**, *78*, 2117.
(12) Richter, D.; Baumgärtner, A.; Binder, K.; Ewen, B.; Hayter, J. B. *Phys. Rev. Lett.* **1981**, *47*, 109.
(13) Dodgson, K.; Semlyen, J. A. *Polymer* **1977**, *18*, 1265.
(14) Allen, G.; Ghosh, R. E.; Higgins, J. S.; Howell, W. S.; Farnoux, B. *Chem. Phys. Lett.* **1977**, *49*, 197.
(15) Information from the Scientific Secretariat, Institut Laue Langevin, BP 156 X, Centre de Tri, 38042 Grenoble, France.
(16) Hayter, J. B. In "Neutron Diffraction"; Dachs, H., Ed.; Springer-Verlag: West Berlin, 1978.
(17) Heidemann, A. In "Neutron Spin Echo"; Mezei, F., Ed; Springer-Verlag: West Berlin, 1980: *Lect. Notes Phys.* Vol. 128.
(18) Howells, W. S. Report RL-81-039; Rutherford Appleton Laboratory: Chilton, Didcot (Oxon.), 1981.
(19) Here the term "configuration" refers to the overall shape of the chain as defined in the phase space of all its space coordinates; therefore, it has nothing to do with the stereochemical configuration. To denote the local molecular shape as defined by

few contiguous internal coordinates we use "conformation" (see also ref 26, footnote at p 15).
(20) Allegra, G. *J. Chem. Phys.* **1978**, *68*, 3600.
(21) Allegra, G. *Macromolecules* **1983**, *16*, 555.
(22) Flory, P. J.; Crescenzi, V.; Mark, J. E. *J. Am. Chem. Soc.* **1964**, *86*, 146.
(23) Allegra, G.; Immirzi, A. *Makromol. Chem.* **1969**, *124*, 70.
(24) Allegra, G.; Calligaris, M.; Randaccio, L. *Macromolecules* **1973**, *6*, 390.
(25) Brückner, S. *Macromolecules* **1981**, *14*, 449. (It should be pointed out that the method based on the continuum of the rotational states, usually referred to as asr (all skeletal rotations), is denoted as ars (all rotational states) both in this paper and in ref 10.)
(26) Flory, P. J. "Statistical Mechanics of Chain Molecules"; Interscience: New York, 1969.
(27) See, e.g.: Massa, D. J.; Schrag, J. L.; Ferry, J. D. *Macromolecules* **1971**, *4*, 210.
(28) Pajot-Augy, E.; Bokobza, L.; Monnerie, L.; Castellan, A.; Bouas-Laurent, H.; Millet, C. *Polymer* **1983**, *24*, 117.
(29) Edwards, C. J. C.; Stepto, R. F. T.; Semlyen, J. A. *Polymer* **1980**, *21*, 781.
(30) Yamakawa, H. "Modern Theory of Polymer Solutions"; Harper and Row: New York, 1971.
(31) Flory, P. J. "Principles of Polymer Chemistry"; Cornell University Press: Ithaca, NY, 1971.
(32) Wignall, G. D.; Ballard, D. G. H.; Shelten, J. *J. Macromol. Sci., Phys.* **1976**, *B12*, 75.
(33) Edwards, S. F.; Freed, K. F. *J. Chem. Phys.* **1974**, *61*, 1189.
(34) Ronca, G., private communication, 1977.
(35) Higgins, J. S.; Ma, K.; Nicholson, L. K.; Hayter, J. B.; Dodgson, K.; Semlyen, J. A. *Polymer* **1983**, *24*, 793.
(36) Berne, B. J.; Pecora, R. "Dynamic Light Scattering with Applications to Chemistry, Biology, and Physics"; Wiley-Interscience: New York, 1976.
(37) Brey, J. J.; Gómez Ordóñez, J. *J. Chem. Phys.* **1981**, *76*, 3260.
(38) Ferry, J. D. "Viscoelastic Properties of Polymers"; Wiley: New York, 1970; Chapter 12.
(39) Akcasu, A. Z.; Higgins, J. S. *J. Polym. Sci., Polym. Phys. Ed.* **1977**, *15*, 1975.
(40) Actually, the upper limit for the virtual disappearance of the effects of hydrodynamic interaction and of excluded volume was set at the lower value $Q = 0.1$ Å^{-1} in the case of polystyrene solutions,[3] which may be attributed to the higher rigidity of this polymer.
(41) Allegra, G.; Benedetti, E.; Pedone, C. *Macromolecules* **1970**, *3*, 727.
(42) Dixon, J. A.; Schiessler, R. W. *J. Phys. Chem.* **1954**, *58*, 430.

Dynamics of Stretched Polymer Chains. 2

Yitzhak Rabin*† and Jan W. Dash‡

La Jolla Institute, Center for Studies of Nonlinear Dynamics,§ La Jolla, California 92037. *Received July 12, 1984*

ABSTRACT: We study the internal modes of an ideal polymer chain that is being stretched by an external force. The effects of the force on the hydrodynamic interaction are investigated by using a preaveraged Oseen tensor approach, for both Gaussian and freely jointed polymer chains.

I. Introduction

Although there have been numerous theoretical investigations of the dynamics of isolated polymers in solution,[1] there were relatively few nonperturbative treatments of the dynamics of non-free-draining, stretched polymer chains.[2-4] In the pioneering work of Peterlin[2,3] polymers in realistic (shear and extensional) flow fields were considered. This has been done at the expense of neglecting the anisotropy of hydrodynamic interaction[2] and treating the dynamics of the lowest mode only[3] (dumbbell model). More recently, in a paper bearing the same title as ours (hereafter referred to as paper 1) Pincus[4] considered the dynamics of a chain stretched by an applied tensile force, focusing on the excluded-volume problem in the limit of high elongations (to which the tensile blob model[5] can be applied).

In view of recent experiments on dilute solutions of elongated chains[6-8] new theoretical investigations in this field are needed. In this work we attempt to study the dynamics of stretched polymer chains following the general approach of paper 1. However, since we do not use the tensile blob model, our results are not confined to the strong stretching limit and we can study the dynamics of ideal polymer coils in both the intermediate and the strong stretching regimes. In addition, we study the effect of the induced asymmetry of hydrodynamic interaction on the relaxation times of the internal modes of the chain. Finally, we investigate the dynamics of real (non-Gaussian) chains, using the $1/n$ expansion about the Gaussian distribution function for the chain[9] (the numerical coefficients in the expansion are taken to be those for a freely joined chain) and linearizing the equations of motion.

In section II, we present the derivation of the spectrum of relaxation times for the polymer modes, taking into acount hydrodynamic interaction via the Oseen tensor and preaveraging the tensor with respect to the distribution function appropriate for a polymer under traction. Closed-form analytic results for the preaveraged Oseen tensor elements are derived in the Appendix. Section III deals with the numerical results for the mode spectrum. The transition from the non-free-draining to the free-draining regimes as the applied tensile force is increased is investigated and is found to be nonmonotonic. The effects of the stretching on the various modes are compared and the stretching-induced asymmetry between longitudinal and transverse modes is studied. Non-Gaussian effects on the spectrum are investigated. In section IV, our main results are summarized and their relevance to some recent experiments is discussed.

II. Relaxation Spectrum

Consider a dilute solution of polymers of length Na where a is the segment size and N is the number of segments in a polymer chain. The viscosity coefficient of the solvent is η_0. This solvent is assumed ideal (ϑ solvent); i.e., we neglect excluded-volume effects.

Balancing the forces acting on the ith segment and neglecting inertial effects and Brownian motion,[1,10] we obtain the equation of motion for the position $\vec{R}_i$ of the ith segment

$$b(\mathrm{d}\vec{R}_i/\mathrm{d}t) = \vec{F}_i^{(e)} + \vec{F}_i^{(h)} \qquad (1)$$

† Permanent address: The Weizmann Institute, Rehovot, Israel.
‡ On leave from CPT2, CNRS, Marseille, France. Present address: Bell Laboratories, Holmdel, NJ 07733.
§ Affiliated with the University of California, San Diego.

0024-9297/85/2218-0442$01.50/0